REPORT DOCUMENTATION PAGE

Form Approved
OMB No. 0704-0188

1. REPORT DATE (DD-MM-YYYY)	2. REPORT TYPE	3. DATES COVERED (From - To)
03/29/2004	Journal	

4. TITLE AND SUBTITLE

Ultraviolet CO Chemiluminescence

5a. CONTRACT NUMBER
F04611-99-C-0025

5b. GRANT NUMBER

5c. PROGRAM ELEMENT NUMBER

6. AUTHOR(S)

Ghanshyam L. Vaghjiani

5d. PROJECT NUMBER
2308

5e. TASK NUMBER
M19B

5f. WORK UNIT NUMBER

7. PERFORMING ORGANIZATION NAME(S) AND ADDRESS(ES)

ERC Incorporated
555 Sparkman Drive
Huntsville, AL 35816-0000

8. PERFORMING ORGANIZATION REPORT NUMBER

9. SPONSORING / MONITORING AGENCY NAME(S) AND ADDRESS(ES)

Air Force Research Laboratory (AFMC)
AFRL/PRS
5 Pollux Drive
Edwards AFB, CA 93524-7048

10. SPONSOR/MONITOR'S ACRONYM(S)

11. SPONSOR/MONITOR'S NUMBER(S)
AFRL-PR-ED-TP-2004-046

12. DISTRIBUTION / AVAILABILITY STATEMENT

Approved for public release; distribution unlimited.

13. SUPPLEMENTARY NOTES
Journal of Chemical Physics

14. ABSTRACT

15. SUBJECT TERMS

16. SECURITY CLASSIFICATION OF:			17. LIMITATION OF ABSTRACT	18. NUMBER OF PAGES	19a. NAME OF RESPONSIBLE PERSON
					Linda Talon
a. REPORT	b. ABSTRACT	c. THIS PAGE	A	37	19b. TELEPHONE NUMBER (include area code)
Unclassified	Unclassified	Unclassified			(661) 275-5283

Ultraviolet CO Chemiluminescence in CH($X^2\Pi$) and CH($a^4\Sigma^-$) Reactions With Atomic Oxygen at 298 K

Ghanshyam L. Vaghjiani

ERC, Inc.
Air Force Research Laboratory
AFRL/PRSA
10 E Saturn Blvd
Edwards AFB, CA 93524
Tel: 661 275 5657
Fax: 661 275 6245
Email: ghanshyam.vaghjiani@edwards.af.mil

Abstract

Production of ultraviolet CO chemiluminescence has been observed for the first time in the gas-phase pulsed laser photolysis of a trace amount of $CHBr_3$ vapor in an excess of O-atoms. O-atoms were produced by dissociation of O_2 or N_2O in a cw-microwave discharge cavity in 2.0 torr of He at 298 K. Temporal profiles of the excited state products that formed in the photo-produced precursor + O-atom (or O_2) reaction were measured by recording their time-resolved chemiluminescence in discrete vibronic bands. The CO 4th Positive transition ($A^1\Pi$, v'=0 $\rightarrow X^1\Sigma^+$, v"=2) near 165.7 nm, the CO Cameron band transition ($a^3\Pi$, v'=0 $\rightarrow X^1\Sigma^+$, v"=1) near 215.8 nm and the OH band transition ($A^2\Sigma^+$, v'=1 $\rightarrow X^2\Pi$, v"=0) near 282.2 nm were monitored in this work to deduce the decay kinetics of the chemiluminescence in the presence of various added substrates. From this the second-order rate coefficient values were determined for reactions of these substrates with the photo-produced precursors. Measured reactivity trends suggest that the prominent precursors responsible for the chemiluminescence are the methylidyne radicals, CH($X^2\Pi$) and CH($a^4\Sigma^-$), whose production requires the absorption of at

least 2 laser photons by the photolysis mixture. The O-atom reactions with brominated precursors, which also form in the photolysis, are shown to play a minor role in the production of the CO chemiluminescence. However, the CBr_2 + O-atom reaction was identified as a significant source for the ultraviolet Br_2 chemiluminescence that was also observed in this work.

1. Introduction

Methylidyne (CH) is the simplest hydrocarbon radical possible. Its reactions are of interest for understanding chemistry in a wide variety of gas-phase environments, such as those found in interstellar clouds, Jovian atmospheres, hydrocarbon combustion chambers, and high altitude Space Shuttle plumes. Its reactivity with numerous molecular species is well documented in the literature [1]. However, studies of its reactions with atomic species are less common. Reactions with O-atoms are of particular interest here.

	ΔH^o_{298K}(kcal mol^{-1})	
$CH(X^2\Pi) + O(^3P) \rightarrow H(^2S) + CO(X^1\Sigma^+)$	(-175.9)	(1)
$\rightarrow HCO(\tilde{X}^2A')$	(-191.6)	(2)
$\rightarrow C(^3P) + OH(X^2\Pi)$	(-21.4)	(3)
$\rightarrow HCO^+(X^1\Sigma^+) + e^-$	(-3.9)	(4)

The overall bimolecular reaction rate coefficient has been determined to be $(9.5 \pm 1.4) \times 10^{-11}$ cm^3 $molec^{-1}$ s^{-1} at 298 K [2]. Channel (4) is thought to be the principal route for primary chemi-ion formation in hydrocarbon flames, and the formyl ion is believed to be involved in soot

production [3]. A branching fraction of 0.0003 at 295 K for channel (4) is deduced from Vinckier's measurement of its reaction rate coefficient of 2.4 x 10^{-14} cm^3 $molec^{-1}$ s^{-1} [4]. Using the 2200 K data of Peeters and Vinckier [5], an activation energy of ~ 1.6 kcal mol^{-1} can be derived for channel (4). Production of carbon-atoms via channel (3) has theoretically been predicted to be negligible at room temperatures because of the significant reaction barrier [6]. Therefore, channels (1) and (2) are expected to be the principal transformation routes. Lin was able to identify the formation of carbon monoxide in channel (1) through its strong 5-μm ir-emissions [7]. However, no absolute product yields have been reported for these two channels. Also, thermodynamically it should be possible to form the electronically excited products, $CO(a^3\Pi, a'^3\Sigma^+, d^3\Delta)$ and $HCO(\tilde{A}^2A'', \tilde{B}^2A', \tilde{C}^2A'')$, in channels (1) and (2), respectively. There are no previous reports of electronic chemiluminescence measurements for channels (1) and (2). It might be that formation of such excited products is facilitated when vibrationally or electronically excited methylidyne is used, as was recently reported in the related (methylidyne + O_2) reaction system [8]. Similarly, $CH(a^4\Sigma^-)$ [9] and $CH(A^2\Delta, B^2\Sigma^-)$ [10] reactions with O-atoms have been shown to enhance chemi-ion formation.

Observations of the $CO(A\rightarrow X)$ and $CO(a\rightarrow X)$ chemiluminescence when $CHBr_3$ is photodissociated at 248 nm in excess O-atoms are reported in this paper. Trends in the decay kinetics of the CO chemiluminescence in various added substrates show that the principal source strength for the radiation is due to the O-atom reactions with the methylidyne radicals in two different electronic states, $CH(a^4\Sigma^-)$ and $CH(X^2\Pi)$. The reactions of brominated radical species such as CBr, CHBr and CBr_2, and C-atoms with O-atoms, in principle, can also produce CO

chemiluminescence, but in the present studies, are of negligible importance. This laboratory work provides evidence for the first time that supports the idea that the interaction of thermospheric O-atoms with carbonaceous species that are present in Space Shuttle plumes could be responsible for part of the far-field ultraviolet emissions observed there [11].

2. Experimental technique

The pulsed-photolysis/discharge flow-tube apparatus used in this work and the experimental procedures used to record the chemiluminescence data has previously been described in detail elsewhere [8,12,13]. A 1% O_2 or 1% N_2O in He mixture was subjected to a cw-microwave discharge in a side-arm cavity to produce O-atoms, which were injected upstream into a flow-tube and carried by excess He into the reaction zone to obtain an O-atom concentration of ~ 1 x 10^{14} molec cm^{-3} in 2.0 torr of the buffer gas. Typically (2-10) x 10^{12} molec cm^{-3} of $CHBr_3$ was also passed into the reaction zone and subjected to a weakly focusing 248-nm laser beam (5-40 mJ/pulse of energy, operating at 10 Hz) to produce low methylidyne concentrations in the detection volume. Ultraviolet chemiluminescence that ensued from the detection zone was monitored perpendicular to the photolyzing beam by imaging the radiation onto the entrance slits of two different scanning spectrometers positioned opposite to each other. The bandpass of the instruments was 2.0 nm, full-width at half-maximum. The photomultipliers used to detect the radiation were configured for single-photon counting detection, the outputs of which were sent to suitable pulse counting units controlled by microcomputers. Spectral scans of the chemiluminescence were obtained by recording the data starting at 20 μs after the laser flash and integrating the signal over the next 100 μs. Typically signals for 20 photolysis flashes

were co-added while the spectrometer was continuously scanned very slowly (0.025 nm s-1). Time-resolved temporal profiles of the chemiluminescence at selected vibronic band positions in CO(A→X) or CO(a→X), and simultaneously in OH(A→X) when O_2 was also present, were recorded using dwell-time resolutions in the range of 2 to 10 μs. 10000 chemiluminescent traces were typically co-added at the computer to improve the signal-to-noise ratio of each of the data sets. The decay kinetics of the chemiluminescence with various added substrates was studied to deduce the corresponding second-order rate coefficient for reaction of the substrate with the precursor radical responsible for generating the excited CO molecules. The N_2O (99.995%) from Alphagaz was used as received. All other material purities were the same as those stated in previous work [8].

3. Results and discussion

3.1 CO-chemiluminescence spectrum

Figure 1 shows a portion of the chemiluminescence spectrum obtained 20 μs after the laser photolysis of $CHBr_3$ vapor in excess O-atoms. The data is well represented by emissions in the 4^{th} Positive and Cameron bands of CO. In this wavelength range, it was confirmed that there was no background chemiluminescence signal from the photolyte/O-atom mixture before the laser flash. It was verified that the laser flash did not induce any coincidental long-lived fluorescence in the detection zone of our quartz reactor by recording a background scan in the absence of $CHBr_3$. Scans were also recorded when only the O_2 flowed into the $CHBr_3$ photolysis zone (i.e., microwave discharge was turned off). In this case, the CO emission

intensity was reduced by ~ 20 times [8], which translates into ~ 80 fold reduction in the source strength when normalized for the reaction rates and the relative concentrations of O-atom and O_2 present in the experiment. This suggests that the O-atom reaction with $CHBr_3$ photolysis product(s) represents the principal source of the observed CO(A) chemiluminescence. The laser fluence dependence of the 165.7-nm CO-chemiluminesence was determined to be (1.79 ± 0.20) in the O-atom experiments, which suggests that the relevant photolysis species are formed via 2-photon absorption processes in our experiments. In this wavelength range, the $CHBr_3$ is thought to photodissociate principally into ($CHBr + Br_2$) and ($CHBr_2 + Br$), with reported channel yields of ~ 0.25 and ~ 0.75, respectively [14,15]. Both the CHBr and the $CHBr_2$ fragments could further absorb a second 248-nm photon within the same initial laser pulse [16] to yield C-atoms, CBr and CH radicals, while the $CHBr_2$ in addition could also yield CHBr and CBr_2 radicals. Only the ground state reaction (C + O) has sufficient reaction enthalpy available for production of CO(A). The other species need to be internally (vibrationally or electronically) excited by at least about 3.8, 9.2, 1.3, and 29.1 kcal mol^{-1}, respectively. Since the yield of CHBr in the initial 1-photon dissociation of the $CHBr_3$ will far exceed that from the subsequent photolysis of $CHBr_2$, our measured quadratic laser fluence dependence of the 165.7-nm CO signal rules out ($CHBr^{\#}$ + O) reaction as the main source for the chemiluminescence (where # denotes excited species). Previously [15], Xu and co-workers were unable to confirm CBr_2 formation in the multi-photon dissociation of $CHBr_3$. Therefore the ($CBr_2^{\#}$ + O) reaction is expected to be a minor source for the CO(A) in our system. There are no reports in the literature on the relative yields of the C-atoms, CBr and CH radicals in $CHBr_3$ photolysis. Some measurements of the vibrational state distribution within the ground state $CH(X^2\Pi)$ are available [17,18], however, no

such studies have been done for the low-lying first excited state CH($a^4\Sigma^-$) which is also known to form in $CHBr_3$ photolysis [19]. The propensity of the doublet state relative to the quartet state in CH formation is also not known. Similar state distribution information for the bromomethylidyne is also not known. To elucidate which of the three carbonaceous species, C-atoms, $CBr^{\#}$ or $CH^{\#}$, is the principal precursor for CO(A) formation, the decay kinetics of the 165.7-nm CO chemiluminescence was studied in various substrates as described below.

3.2 Chemiluminescence decay kinetics

The precursor will react under pseudo-first-order conditions for the case when [precursor] << [O-atom]. Since the CO(A) product of the reaction has a very short radiative lifetime (~ 10 ns), it can be shown that the observed time profile of the associated chemiluminescence in this reaction will follow an exponential decay relationship under our experimental time resolution conditions [8], with a pseudo-first-order decay coefficient of $k' = k_d + k_O[O] + k_{CHBr_3}[CHBr_3] + \Sigma(k_{substrate}[substrate])$. k_d is the first-order rate coefficient for diffusion of the precursor out of the detection zone, and k_O, k_{CHBr_3} and $k_{substrate}$ are the second-order rate coefficient values for the reaction of the precursor respectively with the O-atoms, $CHBr_3$ and the substrates present in the detection zone. The solid circle trace of Figure 2 shows a typical 165.7-nm CO chemiluminescence profile observed immediately after $CHBr_3$ is photodissociated in excess O-atoms. The trace deviates from the anticipated single exponential form, and there are apparently fast and somewhat slower decay components to it. This behavior has been explained previously to result from multiple and independent reactions that produce the CO(A) [8]. This was again confirmed here by adding excess CH_4 (5×10^{15} molec cm^{-3}) to the photolysis reactor and

recording the CO(A) chemiluminescence in otherwise similar experimental conditions. The open circle trace shows this data where there is an initial rapid drop in the chemiluminescent signal followed by what appears to be a single exponential decay. This remaining chemiluminescence must be due to O-atom reaction with either C-atoms or $CH(a^4\Sigma^-)$ since the CH_4 will rapidly (in less than 10 μs) remove only the doublet state of the methylidyne radicals from the photolyzed mixture, while the $[CH(a^4\Sigma^-)]$ and the [C] will remain essentially unperturbed **[8,19,20]**. It is also assumed here that the CH_4 is able to efficiently relax any $CBr^\#$ to the ground state or rapidly remove it by a chemical reaction. Since the CH_4 cannot perturb the [O-atom] and does not significantly alter the CO(A) fluorescence yield in the experiment, direct comparison of the areas under the two traces indicates that the open circle trace represents a source strength of ~ 25% of the total. The signal strength of this source was also shown to have a quadratic dependence on the photolysis fluence employed.

The decay kinetics of this trace was then studied in various added substrates. A value of the second-order rate coefficient for reaction with N_2O was determined to be less than 7×10^{-14} cm^3 $molec^{-1}$ s^{-1} at 298 K in 2.0 torr He. Therefore the (C + O) source is ruled out for this trace as the ($C + N_2O$) reaction rate coefficient is reported to be in the range $(0.8\text{-}1.3) \times 10^{-11}$ cm^3 $molec^{-1}$ s^{-1} **[20-22]**. The other precursor reaction rate coefficients determined under excess CH_4 conditions were $k_{NO} = (3.4 \pm 0.5) \times 10^{-11}$ and $k_{O_2} = (2.2 \pm 0.3) \times 10^{-11}$ cm^3 $molec^{-1}$ s^{-1} for the added substrates NO and O_2, respectively. All rate coefficient uncertainties in this work are reported as 1σ-values that include both precision and estimated systematic errors in the rate determinations. These values are in good agreement with previous ($CH(a^4\Sigma^-)$ + NO) and

($CH(a^4\Sigma^-) + O_2$) reaction rate coefficient measurements [19], and therefore suggest that the chemiluminescence source for the open circle trace of Figure 2 is most likely the ($CH(a^4\Sigma^-) + O(^3P) \rightarrow H(^2S) + CO(A^1\Pi)$) channel, which has a standard reaction enthalpy of ~ - 8.3 kcal mol^{-1}. The energetics of 2-photon production of $CH(a^4\Sigma^-)$ is such that formation of CO(A) will not be possible for its reaction with the NO but, in principle, should be with the N_2O. No overall enhancement in the CO(A) signal was discernable for the range of $[N_2O]/[O]$ employed, therefore the ($CH^{\#} + O$) source term is much stronger than the ($CH^{\#} + N_2O$) term in these set of experiments.

The overall second-order rate coefficient for the ($CH(a^4\Sigma^-) + O(^3P)$) reaction was also determined in this work by varying the [O] by altering the O_2 flow going into the microwave discharge cavity. The absolute O-atom density at the detection zone in the experiment was directly determined before hand in a NO_2-titration run ($O + NO_2 \rightarrow NO + O_2$), whose end-point was photometrically monitored [23]. Figure 3 shows a plot of the pseudo-first-order decay coefficient of the open circle trace in Figure 2 that has been corrected for the contribution from the reaction of undissociated O_2 (i.e., ($k' - k_{O_2}[O_2]_{left}$)) as a function of [O]. Where $[O_2]_{left} = ([O_2]_o - [O]/2)$, and $[O_2]_o$ is the number density of molecular oxygen in the detection zone that would be available in the absence of the microwave discharge. A linear least-squares fit to the slope of the plot yields a value of $k_O = (1.3 \pm 0.2) \times 10^{-10}$ cm^3 $molec^{-1}$ s^{-1} at 298 K in 2 torr He. There is no previous O-atom rate coefficient measurement for reaction with $CH(a^4\Sigma^-)$, but the present value is consistent with that for the reaction with $CH(X^2\Pi)$ previously reported by Messing and co-workers [2] and also by us in this study (see below).

If the CH_4 does not rapidly remove the $CBr^{\#}$, and if the $CH(a^4\Sigma^-)$ does not produce any electronically excited CO in its reaction with O-atoms, then the open circle trace would be attributable to the ($CBr^{\#}$ + $O(^3P) \rightarrow Br(^2P_{3/2})$ + $CO(A^1\Pi)$) reaction channel. The above measured rate coefficients would then represent values for absolute second-order rate coefficients for reactions, respectively, of N_2O, NO, O_2 and O-atoms with the excited bromomethylidyne radical. No comparisons of these values can be made, as previously, only the reaction rate coefficients for the ground state $CBr(X^2\Pi)$ with selected substrates have been reported [24,25]. If the ($CBr^{\#}$ + O) reaction is a significant contributor to the 165.7-nm CO(A) signal, as would be suggested from the open circle trace of Figure 2, we might anticipate the same situation for the production of CO(a), in which case the enthalpy requirement would be satisfied by the presence of ground state bromomethylidyne, whose photolytic yield would surely exceed that of its excited counterparts [17,18]. To resolve these issues, time-resolved CO(a) chemiluminescence decays were studied at 215.8 nm, the wavelength of the Cameron band transition, $CO(a^3\Pi, v'=0 \rightarrow X^1\Sigma^+, v''=1)$. Figure 4 shows a typical result in excess CH_4. Here, the lower open square trace exhibits curvature. (Note that the ground state yield of CBr should not be affected by the addition of CH_4 since both its H-abstraction and Br-substitution reaction are endothermic.) From initial exponential fits to the decay for the open square trace, a value of $k_{O_2} = (2.1 \pm 0.3) \times 10^{-11}$ cm^3 $molec^{-1}$ s^{-1} was determined. This suggests that the ($CBr(X^2\Pi)$ + O) reaction cannot be a dominant source for the observed CO(a) chemiluminescence since previous reports for the ($CBr(X^2\Pi)$ + O_2) reaction rate coefficient lie in the range $(1.5\text{-}2.2) \times 10^{-12}$ cm^3 $molec^{-1}$ s^{-1} [24,25]. The above measured O_2 rate coefficient and the ground state

($CHBr + O_2$) rate coefficient previously estimated to be 1.7×10^{-14} cm^3 $molec^{-1}$ s^{-1} [26] also rules out ($CHBr + O$) as being the main source for CO(a). Because we have been able to show in CBr_4/O-atom photolysis [27] that CBr can react with O-atoms to produce excited CO, it is concluded that in $CHBr_3$ photolysis, the relative yield of the bromomethylidyne radicals must be very small compared to that of $CH(a^4\Sigma^-)$ or $CH(X^2\Pi)$. Therefore the lower traces of Figures 2 and 4 are principally due to the ($CH(a^4\Sigma^-) + O(^3P)$) source reaction.

The small curvature in the lower trace of Figure 4 can either be explained by assuming that there are minute CO(a) contributions from O-atom reactions with CBr, CBr_2 and CHBr, or that there is weak emission from another species that happens to radiate in the same observation window as that used to follow the 215.8-nm CO(a) chemiluminescence. In either case, the responsible precursor has a lower reactivity with O_2 than does the $CH(a^4\Sigma^-)$ radical. Similar observations were seen when the spectrometer bandpass was set to observe the strong $OH(A \rightarrow X)$ emission in the $(1 \rightarrow 0)$ band near 282.2 nm when $CHBr_3$/O-atom/O_2 mixtures were photolyzed. Figure 5 shows typical chemiluminescence decays observed in the absence of O-atoms (i.e., microwave discharge off); the x trace and the open triangle trace is for $[CH_4] = 0$, and 5.0×10^{15} molec cm^{-3}, respectively. When O-atoms are injected (i.e., microwave discharge on), the solid square and the open square traces were obtained, respectively for $[CH_4] = 0$, and 5.0×10^{15} molec cm^{-3}.

The x trace represents the time profile of the strong OH(A) chemiluminescence predominantly due to the occurrence of the O_2 reaction with $CH(X^2\Pi)$ and to a small extent

with $CH(a^4\Sigma^-)$ [8]. Upon adding excess methane a fast drop in the OH(A) chemiluminescence is observed which would be consistent with the fast removal of any $CH(X^2\Pi)$ present in the photolyzed mixture [8,19]. The resulting open triangle trace then represents the time profile of the OH(A) chemiluminescence due to only the $(CH(a^4\Sigma^-) + O_2)$ reaction. By adding various amounts of N_2O to the experiments for these two conditions, the rate coefficient values of $k_{N_2O} = (5.1 \pm 0.9) \times 10^{-11}$ and $< 1 \times 10^{-13}$ cm^3 $molec^{-1}$ s^{-1} for N_2O reactions with $CH(X^2\Pi)$ and $CH(a^4\Sigma^-)$ were obtained, respectively. In principle, Cameron band chemiluminescence produced in these O_2 reactions would also be detected at this spectrometer setting, e.g., in the weak $CO(a^3\Pi, v'=2 \rightarrow X^1\Sigma^+, v''=8)$ band, however, its contribution to the observed signal in the open triangle trace would be severely suppressed due to efficient CO(a) fluorescence quenching by the excess CH_4. The solid square trace shows that the initial time profile is not affected much when O-atoms are added to the O_2 flow (x trace), however, the occurrence of additional chemiluminescence in the system is clearly discernable at long reaction times. Its yield and decay rate are much smaller. This chemiluminescence is neither quenched nor its decay kinetics affected significantly when excess CH_4 is added (open square trace). Therefore an O-atom reaction with a precursor, Y, which predominantly yields an electronically excited species other than CO(a) must be responsible for the signal in this time region. However, in the early part (time $< \sim 200$ μs), the solid square trace does get affected by the addition of CH_4. The initial portion of this signal is predominantly from OH(A) chemiluminescence which can only come from the methylidyne reactions with the O_2. The fast drop (within 20 μs) in the open square trace is therefore due to the removal of $CH(X^2\Pi)$ from the system, while the phenomenological

curved decay in the 20-100 μs range represents comparable chemiluminescence signals from ($CH(a^4\Sigma^-) + O$) and (Y + O) reactions.

A kinetics study of the precursor, Y, was carried out in order to elucidate its identity and that of the electronically excited product, $Z^\#$, formed in its reaction with atomic oxygen. For a fixed amount of [O-atom] present in the experiments, the solid square traces of Figure 5 were determined at various different O_2 concentrations in the range (2-10) x 10^{14} molec cm^{-3}. Exponential fits were performed in the initial fast decaying part, and in the slow decaying part at very long times to extract the values for the pseudo-first-order decay coefficients. Second-order plots of these gave k_{O_2} = (3.4 ± 0.6) x 10^{-11} and < 1 x 10^{-13} cm^3 $molec^{-1}$ s^{-1} for the O_2 reactions with $CH(X^2\Pi)$ and Y, respectively. Then by varying the O-atom concentration by known amounts, an analysis similar to that of Figure 3 was performed for both regions of the trace. This gave k_O = (1.1 ± 0.2) x 10^{-10} and (5.9 ± 0.9) x 10^{-11} cm^3 $molec^{-1}$ s^{-1} for the O-atom reactions with $CH(X^2\Pi)$ and Y, respectively. Our ($CH(X^2\Pi)$ + O) reaction rate coefficient value is in good agreement with the one previous determination [2] and similar to that for the ($CH(a^4\Sigma^-)$ + O) reaction. The CH_4 + Y reaction rate coefficient was also estimated to be < 7 x 10^{-14} cm^3 $molec^{-1}$ s^{-1}. Since ($HCBr_2$ + O) and (HCBr + O) reactions are both endothermic for the production of electronically excited OH, the slowly decaying chemiluminescence signal in Figure 5 cannot be due to OH(A) emissions. A spectral scan in this wavelength vicinity was therefore recorded as described below in order to determine the identity of the emitter $Z^\#$.

3.3 Br_2-chemiluminescence spectrum and decay kinetics

The spectral scan was recorded in excess methane conditions with sufficiently high [O_2] and at a long delay time after the initial laser flash. The O_2 served to increase the rate of consumption of the CH($a^4\Sigma^-$) while the methane served to rapidly remove the CH($X^2\Pi$) through its fast reaction with it and reduce the Cameron band fluorescence quantum yield by quenching the CO(a) produced in these reactions. The long delay time further served to reduce the detection yield of the CO(a) and OH(A) products relative to Z# produced in the photolysis. Since the signal level for the slowly decaying Z# chemiluminescence is less than ~ 5% of the fast decaying components (see Figure 5), the spectral data this time was recorded in steps of 1 nm, and at each spectrometer setting, the signal between 300 and 1000 μs was integrated and co-added for 10000 laser flashes to improve the signal-to-noise ratio of the data. Figure 6 shows the result. The x trace is the pre-trigger background spectrum obtained before the laser fires. The solid circle trace is the background subtracted spectrum obtained in the photolysis run. The apparent noise in the data set between each spectrometer setting is probably statistical in nature as a result of integrating the weakly decaying chemiluminescence signal in the photolysis. Nevertheless, a pronounced feature at ~ 290 nm for the Z# species is seen. Weaker continuous emissions at shorter wavelengths with possibly diffuse bands are also discernable. This spectrum clearly shows that when a spectrometer setting of 282.2 nm is chosen to study the OH(A) chemiluminescence as in Figure 5, there will be a phenomenological curvature in the trace because of the simultaneous detection of the Z# radiation. Similar spectra for both the background (no photolysis) and in the photolysis runs were also observed when CBr_4 [27] was used instead of $CHBr_3$ under excess O-atom conditions. This suggests that in both cases the

photolysis in excess O-atoms yields the same precursor, Y, which reacts further with the O-atoms to yield Z#. Furthermore, the species Y, is also generated in the absence of any photolysis when CBr_4 [27] or $CHBr_3$ is oxidized in excess O-atoms. We identify the observed strong feature at ~ 290 nm to be the Br_2 (D→A) electronic transition in the (0→0) band [28] with the weaker, short-wavelength diffuse features associated with emissions possibly (from other nearby states) to the ground electronic state. The intensity of this chemiluminescence signal had a (1.30 ± 0.26) dependence on the laser fluence employed. This suggests that the Y precursor is formed in the detection zone through a 1-photon absorption process. Figure 7 shows the fluence dependence of the 289.9-nm signal. A study of the decay kinetics of the 289.9-nm chemiluminescence in excess CH_4 in varying amounts of molecular oxygen and O-atom was performed to yield second-order reaction rate coefficient values of $< 9 \times 10^{-14}$ and $(5.4 \pm 1.0) \times 10^{-11}$ cm^3 $molec^{-1}$ s^{-1} in 2.0 torr He and at 298 K for the reaction of the precursor Y with O_2 and O-atoms, respectively. The Y + CH_4 reaction rate coefficient was again estimated to be $< 7 \times 10^{-14}$ cm^3 $molec^{-1}$ s^{-1}. It is to be noted that these values are similar to the ones obtained when the slowly decaying 282.2-nm chemiluminescence of Figure 5 was analyzed. Since the production of $Br_2(D)$ in the fast O-atom reaction requires the precursor Y to have at least 2 bromine atoms in its molecular formula, we interpret our above kinetics data as that for Y being the CBr_2 species. Note that the O-atom reactions with $CHBr_2$# and with CBr_3# (if directly formed in $CHBr_3$ photolysis) are both endothermic for the production of $Br_2(D)$. There are no literature data available for comparison; however, our measured rate coefficients for CBr_2 are consistent with the trends exhibited by its homologous counter parts [29].

3.4 Reaction mechanisms

3.4.1 Production of CBr_2 and $Br_2(D)$: The $Br_2(D \rightarrow A)$ emissions seen in our $CHBr_3$/O-atom cold flame in the absence of any photolysis can be rationalized by the following sequence of reactions in excess O-atoms:

	ΔH^o_{298K}(kcal mol-1)	
$CHBr_3 + O \rightarrow OH + CBr_3$	(-8.3)	(5)
$CBr_3 + O \rightarrow CBr_2 + BrO$	(-0.2)	(6)
$CBr_2 + O \rightarrow CO + Br_2$	(-156.0)	(7)

The bromoform undergoes slow oxidation principally via the H-abstraction reaction (5) [27]. The tribromomethyl radical product undergoes facile oxidation by the O-atoms, which in its Br-abstraction reaction channel (6) yields the dibromomethylene radical. This then rapidly reacts with the O-atoms, and in the very exothermic reaction channel (7), molecular elimination takes place to give (CO + Br_2). There is sufficient reaction enthalpy available in this process to electronically excite the bromine molecule up to the D-state. The $Br_2(D)$ has a reported radiative lifetime of ~ 10 ns [30], and is known to relax principally via the (D→A) electronic emission near 289.9 nm. Electronically excited carbon monoxide up to the a-state can also form in this reaction. Evidence for this is provided elsewhere [27], where we report very weak CO(a) chemiluminescence spectra in the 180-260 nm range for $CHBr_3$/O-atom and CBr_4/O-atom cold flames. It is argued that in these cold flames, CBr production will be negligible (relative to

CBr_2), and therefore the ($CBr + O \rightarrow Br + CO(a)$) reaction does not play a major role in the production of the observed CO(a) chemiluminescence. Also, since CH formation should not be possible in the $CHBr_3$/O-atom flame, the ($CH + O \rightarrow H + CO(a)$) reaction cannot be used here to explain these emissions.

The fast rise in the $Br_2(A)$ signal in Figure 7 suggests that when a $CHBr_3$/O-atom mixture is photolyzed, there is photolytic production of CBr_2. However, previous work [15] had failed to detect any dibromomethylene formation in $CHBr_3$ photodissociation. Therefore, Figure 7 provides first evidence that perhaps a very small fraction of the photolysis may indeed be proceeding via the ($CHBr_3 + h\nu \rightarrow CBr_2 + HBr$) channel to directly yield CBr_2. Furthermore, the data of Figure 7 also reveals that the rate of decay of the chemiluminescence is not quite exponential, i.e., the initial decay rate is somewhat suppressed. Therefore, a second photochemical source for CBr_2 formation may also be operative. A possible route for this would be the ($CHBr_2 + O \rightarrow CBr_2 + OH$) reaction, where the dibromomethyl radical is produced in the initial photolysis of the $CHBr_3$. Furthermore, since the CBr_3 radical, formed in reaction (5) will also be present in the detection zone, its photolysis ($CBr_3 + h\nu \rightarrow CBr_2 + Br$) may generate more CBr_2. The relative importance for these three processes has not been ascertained in this work, however, from the huge signal in the upper trace of Figure 6 relative to that of the lower trace, it can be shown that the first two sources discussed above should dominate. In any case, the observed linear dependence of the 289.9-nm chemiluminescence intensity on the fluence of the photolysis laser is consistent with the production of CBr_2 via any combination of the above three photolytic mechanisms. It also implies that 2-photon absorption

processes to generate CBr_2 via $CHBr_3 + h\nu \rightarrow CHBr_2 + Br$, followed by $CHBr_2 + h\nu \rightarrow CBr_2 + H$, or $CHBr_3 + h\nu \rightarrow CBr_3 + H$, followed by $CBr_3 + h\nu \rightarrow CBr_2 + Br$ are relatively unimportant compared to the above mechanisms. This further suggests that the primary quantum yields for CBr_3 and CBr_2 production, respectively, in 1-photon photolysis of $CHBr_3$ [31] and $CHBr_2$ are very small, and therefore H-atom production must also be negligible.

3.4.2 Production of CO(A and a) and CH(X and a): Our measured CO(A) chemiluminescence decay trends with various added substrates indicate that the prominent source for CO(A) is the $CH(a^4\Sigma^-) + O$ reaction when excess CH_4 is present in the photolysis mixture. The 2-photon generation of the quartet methylidyne radical can be summarized as the process: $CHBr_3 + 2h\nu(248\ nm) \rightarrow CH(a^4\Sigma^-) + Br_2 + Br$; $\Delta H^o_{298K} = \sim -43.0$ kcal mol^{-1}. On removing the methane, there is an enhancement in the CO(A) signal by ~ 4 times, however, the chemiluminescence decay is no longer exponential. This is because the doublet methylidyne radical also formed in the photolysis: $CHBr_3 + 2h\nu(248\ nm) \rightarrow CH(X^2\Pi) + Br + Br_2$ (or Br + Br); $\Delta H^o_{298K} = \sim -60.5$ (or ~ -14.5) kcal mol^{-1} is now available to participate in the O-atom reaction. In this case, the production of CO(A) can only be possible if the doublet methylidyne radical processes at least 9.2 kcal mol^{-1} of internal energy. Since any rotationally excited doublet methylidyne will rapidly thermalize in the 2 torr He buffer gas, the presence of vibrationally excited species such as $CH(X^2\Pi, v''\geq 2)$ is necessary to explain the top trace in Figure 2. Previously [32] it has been shown that both the v"=1 and v"=2 vibrational states are not efficiently quenched by helium. It can be shown that in the present experiments, the reactions of O-atoms and that of any added substrate will compete with the slow quenching by

the He in the removal of these species. The areas of the traces in Figure 2 only provide values for the phenomenological source strengths for CO(A) chemiluminescence, since information on the integrated yield of $CH(a^4\Sigma^-, v'\geq 0)$ relative to $CH(X^2\Pi, v''\geq 2)$ is not available in the 2-photon dissociation of $CHBr_3$, nor is there data available on the state-specific branching fractions for the production of CO(A) in their reactions with the O-atoms. As there is pronounced phenomenological curvature in the top trace of Figure 2, we did not attempt to measure the second-order rate coefficients for the initial decay of the chemiluminescence in the added substrates NO, O_2 and N_2O, since such an analysis would under estimate the true value of their reaction rate coefficients with $CH(X^2\Pi, v''\geq 2)$.

The overall bimolecular rate coefficients of O-atom reactions with $CH(X^2\Pi)$ and $CH(a^4\Sigma^-)$ are very large and similar in value. Formation of ground state ($CO(X^1\Sigma^+) + H(^2S)$) products (or ($CO(A^1\Pi) + H(^2S)$) in the system is spin allowed and expected to proceed via an addition/elimination reaction mechanism on a doublet potential energy surface. Formation of the ($CO(a^3\Pi + H(^2S)$) products could proceed via a doublet and/or a quartet potential energy surface. The lifetime of the energized intermediate(s), {HCO}*, will be very short of the order of a vibrational period. If dissociation directly produces CO in any of the energetically allowed states, the corresponding ultraviolet chemiluminescence signals in the reaction will have growth maxima that will be determined by the experimental lifetime, τ, of the emitting products. The distinct rise in the top trace of Figure 2 for the 165.7-nm chemiluminescence signal associated with the $CO(A^1\Pi, v'=0)$ emitter, whose radiative lifetime is known to ~ 10 ns, suggests that this product does not exclusively form directly from the energized {HCO}* intermediate. This was confirmed by recording the CO(A) chemiluminescence trace with a higher time resolution of 2

μs where a large instantaneous signal followed by a small rise that typically maximized at ~ 10 μs was observed. This implies that, in addition, there are a set of other CO states that are the initial products from {HCO}* dissociation which then undergo very fast intersystem crossing to yield $CO(A^1\Pi)$. Most likely these are the $(a^3\Pi)$ meta-stable states near v'=11 that cross over to the $(A^1\Pi)$ vibrational manifold through collisions with excess O-atoms/O_2 (and buffer gas [33]) via near-resonant energy transfer processes, see Figure 8. The nearby vibrational manifold of the $(a'^3\Sigma^+)$ and $(d^3\Delta)$ states could also populate the $A(^1\Pi)$ system through spin-orbit and rotation-electronic interactions. However, these states have high Einstein transition probabilities for spontaneous decay to the lower vibrational levels of the $(a^3\Pi)$ state and therefore should principally decay via visible-ir emissions, with radiative lifetimes in the few microsecond range. Similarly, the position of the maximum in the solid square trace of Figure 4, is consistent with the direct formation (and/or through the above cascading mechanism) of the meta-stable $CO(a^3\Pi, v'=0)$ state (radiative lifetime, τ_r = ~ 7 ms) that is undergoing rapid quenching by the excess O-atoms and O_2 [34]. Future high-level *ab-initio* theoretical calculations on the ($CH + O \rightarrow CO + H$) system should offer further insight about the potential energy surface(s), the transition state(s), the reaction intermediate(s), and the reaction dynamics involved. It is to be noted that in the related ($CH + O_2 \rightarrow CO + OH$) reaction, the initial energized reaction adduct, {OOCH}*, undergoes fast rearrangement/dissociation via a four-center intermediate to directly yield the OH(A) product since no rise in the 282.2-nm signal is seen in the solid square trace of Figure 5.

Hydrocarbon flame emissions due to electronically excited formyl radicals could not be positively identified in the photolysis. The $(0,0,0 \rightarrow 0,0,0)$ band origins for the $(\tilde{B} \rightarrow \tilde{X})$ and $(\tilde{C} \rightarrow \tilde{X})$ transitions are near 258.2 and 241.3 nm, and therefore lie within the strong CO Cameron band emissions. Our 220-280 nm spectral scans of the chemiluminescence in $CHBr_3$/O-atom photolysis were very similar to those obtained in CBr_4/O-atom photolysis in which $HCO(\tilde{B}, or\ \tilde{C})$ cannot form. In both cases, all the observed vibronic peaks could be assigned to $CO(a \rightarrow X)$ transitions [27]. Therefore in the present experiments, the $\{HCO\}^*$ intermediate cannot be stabilized efficiently to yield any significant amounts of electronically excited formyl radicals.

3.4.3 Check for $CH(a^4\Sigma^-) \rightarrow CH(X^2\Pi)$ collisional processes: In the above discussions, the phenomenological curvatures in the solid circle trace of Figure 2 and in the x trace of Figure 5 were explained by suggesting that reactions of both $CH(X^2\Pi)$ and $CH(a^4\Sigma^-)$ independently contribute to the production of the excited products. However, an alternate mechanism needs to be considered in which the $CH(a^4\Sigma^-)$ does not directly produce any excited products in its reactions, but rather slowly generates more $CH(X^2\Pi)$ in the system after the photolytic pulse. Through collisions with excess buffer gas it could well be that the $CH(a^4\Sigma^-, v'=0)$ undergoes intersystems crossing to produce $CH(X^2\Pi, v'' \leq 2)$. In this case the [CH(X)] temporal profile would be of the form: $[CH(X)]_o e^{-k_{CH(x)}.t} + k_{He}[He][CH(a)]_o(e^{-k_{CH(a)}.t} - e^{-k_{CH(x)}.t})/(k_{CH(x)} - k_{CH(a)})$. Where $[CH(X)]_o$ and $[CH(a)]_o$, respectively, are the initial photolytic yields of the doublet and quartet methylidyne radicals, with $k_{CH(x)}$ and $k_{CH(a)}$ as their corresponding pseudo-first-order decay coefficients, and k_{He} as the second-order rate coefficient for He collisions with

CH(a) that lead to CH(X) production. This type of a [CH(X)] temporal profile will also lead to non-exponential chemiluminescence decay signals for the excited state species formed in CH(X) reactions, and in excess [CH_4] conditions the decay rate of the remaining chemiluminescence signal will provide a measure of the reactivity of CH(a) with any added substrate. If this alternate scheme predominates in our photolysis, both the chemiluminescence yield and its decay rate will be dependent on the He pressure. To test for this, the related reaction of NO with methylidyne radicals was studied in 5 x 10^{15} molec cm^{-3} of CH_4 at two different He pressures of 2.0 and 22.0 torr. The 336.2-nm emission from the $NH(A^3\Pi)$ product [35] was monitored at constant [NO], [$CHBr_3$] and laser fluence conditions. The higher pressure experiment produced no enhancement in the chemiluminescence signal. An upper limit of $k_{He} < 1 \times 10^{-14}$ cm^3 $molec^{-1}$ s^{-1} was estimated for the reaction rate coefficient for removal of CH(a) by He. These results imply that the imidogen radical can also directly form in the (CH(a) + NO) reaction through a short lived four-center reaction intermediate, and that the conversion of CH(a) to CH(X) in the present work plays a minor role in producing the observed non-exponential chemiluminescence decay traces. The k_{NO} rate coefficients for (CH(X) + NO) and (CH(a) + NO) reactions were also determined from the decays of the 336.2-nm traces. At 298 K, the k_{NO} values were, respectively, $(1.8 \pm 0.3) \times 10^{-10}$ and $(4.2 \pm 0.7) \times 10^{-11}$ cm^3 $molec^{-1}$ s^{-1}, and were shown to be independent of the He pressure employed. These values are consistent with previous literature numbers [19,35,36].

4. Conclusions

Strong ultraviolet chemiluminescence was observed in the laser photolysis of $CHBr_3$/O-atom/O_2 mixtures in 2 torr of He. Spectral scans in the 120-300 nm wavelength range showed CO(A), CO(a), Br_2(D) and OH(A) to be the prominent emitters. The photo-products of $CHBr_3$ photolysis react with O-atoms to generate CO(A), CO(a) and Br_2(D), and react with O_2 to generate OH(A). The identities of these photo-products were established by studying the laser fluence dependence of the chemiluminescent intensities, and by carrying out kinetic trend analysis on how the chemiluminescent decay behaved in various added substrates, and by making comparisons of the observed second-order rate coefficient data to literature values. The methylidyne radicals ($CH(X^2\Pi)$ and $CH(a^4\Sigma^-)$ were thereby identified to be involved in the production of CO(A), CO(a) and OH(A), and the dibromomethylene radical (CBr_2) in the production of Br_2(D). The present work provides evidence for the first time that supports the idea that the interaction of thermospheric O-atoms with carbonaceous species of Space Shuttle plumes could be responsible for part of the far-field ultraviolet emissions observed there[11].

Acknowledgment

Funding for this work was provided by the Air Force Office of Scientific Research under Contract # F04611-99-C-0025 with the Air Force Research Laboratory, Edwards AFB, CA 93524.

References

(1) D. L. Baulch, C. J. Cobos, R. A. Cox, C. Esser, P. Frank, Th. Just, J. A. Kerr, M. J. Pilling, J. Troe, R. W. Walker and J. Warnatz, J. Phys. Chem. Ref. Data 21 (1992) 411.

(2) I. Messing, S. V. Filseth, C. M. Sadowski and T. Carrington, J. Chem. Phys. 74 (1981) 3874.

(3) H. F. Calcote, 8th Symposium (International) on Combustion (Williams & Williams, 1962) p. 184.

(4) C. Vinckier, J. Chem. Phys. 83 (1979) 1234.

(5) J. Peeters and C. Vinckier, 15th Symposium (International) on Combustion (The Combustion Institute, Pittsburgh, 1975) p. 969.

(6) J. N. Murrell and J. A. Rodriguez, J. Mol. Struc. Theochem. 139 (1986) 267.

(7) M. L. Lin, Int. J. Chem. Kinet. 6 (1974) 1.

(8) G. L. Vaghjiani, J. Chem. Phys. 119 (2003) 5388.

(9) D. E. Phippen and K. D. Bayes, Chem. Phys. Lett. 164 (1989) 625.

(10) T. A. Cool and P. J. H. Tjossem, Chem. Phys. Lett. 111 (1984) 82.

(11) R. A. Viereck, E. Murad, D. J. Knecht, C. P. Pike, L. S. Bernstein, J. B. Eglin and A. L. Broadfoot, J. Geophys. Res. A101 (1996) 5371.

(12) G. L. Vaghjiani, J. Phys. Chem. A105 (2001) 4682.

(13) G. L. Vaghjiani and A. R. Ravishankara, J. Phys. Chem. 93 (1989) 1948.

(14) K. D. Bayes, D. W. Toohey, R. R. Friedl and S. R. Sander, J. Geophys. Res. D108 (2003) 4095.

(15) D. Xu, J. S. Francisco, J. Huang and W. M. Jackson, J. Chem. Phys. 117 (2002) 2578.

(16) J. Lindner, K. Ermisch and R. Wilhelm, Chem. Phys. 238 (1998) 329.

(17) S. Okada, K. Yamasaki, H. Matsui, K. Saito and K. Okada, Bull. Chem. Soc. Jpn. 66 (1993) 1004.

(18) C. Mehlmann, M. J. Frost, D. E. Heard, B. J. Orr and P. F. Nelson, J. Chem. Soc., Faraday Trans. 92 (1996) 2335.

(19) Z. Hou and K. D. Bayes, J. Phys. Chem. 97 (1993) 1896.

(20) D. Husain and L. J. Kirsch, Trans. Faraday Soc. 67 (1971) 2025.

(21) D. Husain and A. N. Young, J. Chem. Soc. Faraday Trans. 2 71 (1975) 525.

(22) G. Dorthe, Ph. Caubet, Th. Vias, B. Barrere and J. Marchais, J. Phys. Chem. 95 (1991) 5109.

(23) G. L. Vaghjiani, J. Chem. Phys. 104 (1996) 5479.

(24) R. S. McDaniel, R. Dickson, F. C. James and O. P. Strausz, Chem. Phys. Lett. 43 (1976) 130.

(25) A. J. Marr, T. J. Sears and P. B. Davies, J. Mol. Spectrosc. 184 (1997) 413.

(26) R. Wagener and H. Gg. Wagner, Z. Phys. Chem. 175 (1992) 9.

(27) G. L. Vaghjiani, Chem. Phys. Lett. Work to be published.

(28) K. P. Huber and G. Herzberg, *Molecular Spectra and Molecular Structure IV. Constants of Diatomic Molecules,* Van Nostrand Reinhold, New York, 1979.

(29) *17. NIST Chemical Kinetics Database: Version 2Q98* (Standard Reference Data Program National Institute of Standards and Technology, Gaithersburg, MD 1998) and references therein.

(30) D. I. Austin, R. J. Donovan, A. Hopkirk, K. P. Lawley, D. Shaw and A. J. Yencha, Chem. Phys. 118 (1987) 91.

(31) K. McKee, M. A. Blitz, K. J. Hughes, M. J. Pilling, H.-B. Qian, A. Taylor and P. W. Seakins, J. Phys. Chem. A107 (2003) 5710.

(32) M. A. Blitz, M. Pesa, M. J. Pilling and P. W. Seakins, Chem. Phys. Lett. 322 (2000) 280.

(33) C. Kittrell, S. Cameron, L. Butler and R. W. Field, J. Chem. Phys. 78 (1983) 3623.

(34) W. Felder, W. Morrow and R. A. Young, Chem. Phys. Lett. 15 (1972) 100.

(35) D. A. Lichtin, M. R. Berman and M. C. Lin, Chem. Phys. Lett. 108 (1984) 18.

(36) A. Bergeat, T. Calvo, N. Daugey, J. C. Loison and G. Dorthe, J. Phys. Chem. A102 (1998) 8124.

Figure captions

Figure 1 A portion of the CO-chemiluminescence spectrum obtained 20 μs immediately after 248-nm laser photolysis of $CHBr_3$ in the presence of an excess of O-atoms at 298 K and in 2.0 torr of He pressure. The O-atoms were produced by dissociation of N_2O in a cw-microwave discharge cavity. The observed vibronic emissions can be assigned to the 4^{th} Positive bands, $CO(A \rightarrow X)$ and the Cameron bands, $CO(a \rightarrow X)$. The data has not been normalized for any variation in the photon detection efficiency of our photomultiplier over this wavelength region.

Figure 2 Time-resolved 165.7-nm CO-chemiluminescence traces observed immediately after 248-nm photolysis of $CHBr_3$ (5.0×10^{12} molec cm^{-3}) in the presence of O_2 (1.1×10^{14} molec cm^{-3}) and O-atoms (2.0×10^{13} molec cm^{-3}) at 298 K and in 2.0 torr of He pressure. The solid circle trace was obtained in the absence of methane and the open circle trace was obtained in the presence of methane (5.0×10^{15} molec cm^{-3}). The time resolution for recording the

signal was 10 μsec. 10000 temporal profiles were co-added to improve the signal-to-noise ratio of the chemiluminescence traces. The line is an exponential fit (after 30 μs) to the data points of the open circle trace. The magnitude of the slope yields a value for k'.

Figure 3 A plot of ($k' - k_{O_2}[O_2]_{left}$) as a function of [O] for experiments in which $CHBr_3$ (7.0×10^{12} molec cm^{-3}) was photodissociated in the presence of CH_4 (5.0×10^{15} molec cm^{-3}) in 2.0 torr of He buffer gas at 298 K with a known excess of O-atoms and O_2. The magnitude of the slope yields a value for the ($CH(a^4\Sigma^-) + O$) reaction rate coefficient.

Figure 4 Time-resolved 215.8-nm chemiluminescence traces observed immediately after 248-nm photolysis of $CHBr_3$ (1.0×10^{13} molec cm^{-3}) in the presence of O_2 (3.7×10^{14} molec cm^{-3}) and O-atoms (7.0×10^{13} molec cm^{-3}) at 298 K and in 2.0 torr of He pressure. The solid square trace was obtained in the absence of methane and the open square trace was obtained in the presence of methane (5.0×10^{15} molec cm^{-3}). The time resolution for recording the signal was 10 μsec. 10000 temporal profiles were co-added to improve the signal-to-noise ratio of the chemiluminescence traces.

Figure 5 Time-resolved 282.2-nm chemiluminescence traces observed immediately after 248-nm photolysis of $CHBr_3$ (6.0×10^{12} molec cm^{-3}) at 298 K in He (2.0 torr). The x trace is obtained with O_2 (8.8×10^{14} molec cm^{-3}) present but in the absence methane, while the open triangle trace is obtained for the same amount of O_2 but with methane (5.0×10^{15} molec cm^{-3}) also present. The open squares trace is obtained when O-atoms (5.0×10^{13} molec cm^{-3}) are

injected into the apparatus with both O_2 and methane also present, and the solid square trace is obtained with the same amounts of O-atoms and O_2 present but in the absence of methane. The time resolution for recording the signal was 10 μsec. 10000 temporal profiles were co-added to improve the signal-to-noise ratio of the chemiluminescence traces.

Figure 6 The ultraviolet chemiluminescence spectrum (solid circle) obtained 300 μs after 248-nm laser photolysis of $CHBr_3$ in excess O-atoms produced in a N_2O microwave discharge, with O_2 (1.0×10^{15} molec cm^{-3}) and CH_4 (5.0×10^{15} molec cm^{-3}) present in 2.0 torr He at 298 K. The x trace spectrum is obtained when the laser is off. The strong Br_2 (D→A) electronic emission at ~ 289.9 nm is clearly identified. Continuous emissions at shorter wavelengths with possibly weaker diffuse band(s) can also be discerned. The data has not been normalized for any variation in the photon detection efficiency of our photomultiplier over this wavelength region.

Figure 7 289.9-nm time-resolved chemiluminescence traces obtained in the photolysis of $CHBr_3$ (7.0×10^{12} molec cm^{-3}) at four different 248-nm laser fluences. The O-atoms (9.0×10^{13} molec cm^{-3}) were generated by discharging N_2O (2.2×10^{14} molec cm^{-3}) in a microwave cavity. The data were recorded in the presence of excess CH_4 (5.0×10^{15} molec cm^{-3}) in 2.0 torr He at 298 K. The CH_4 helps to minimize the detection of any OH(A) emissions in the red wing of its (1→0) band and any CO(a) emissions such as in the (6→12) band at this wavelength, since it (1) rapidly scavenges any $O(^1D)$ formation from N_2O photolysis and thus minimizes O_2 formation, (2) rapidly removes the $CH(X^2\Pi)$ formed in $CHBr_3$ photolysis, and (3) efficiently quenches the CO(a) fluorescence signal. The lines are exponential fits to the data set. The inset

shows the plot of the logarithmic of the integrated intensity (i.e., the area) of these curves as a function of the logarithmic of the laser fluence used.

Figure 8 A schematic energy diagram for the (CH + O) reaction system. The labels refer to the electronic and the vibrational levels of the radical species. Only those levels relevant to the present discussion are shown. The energy range of the intermediate is indicated by the min/max limits possible as a result of 2-photon dissociation of $CHBr_3$.

Figure 1

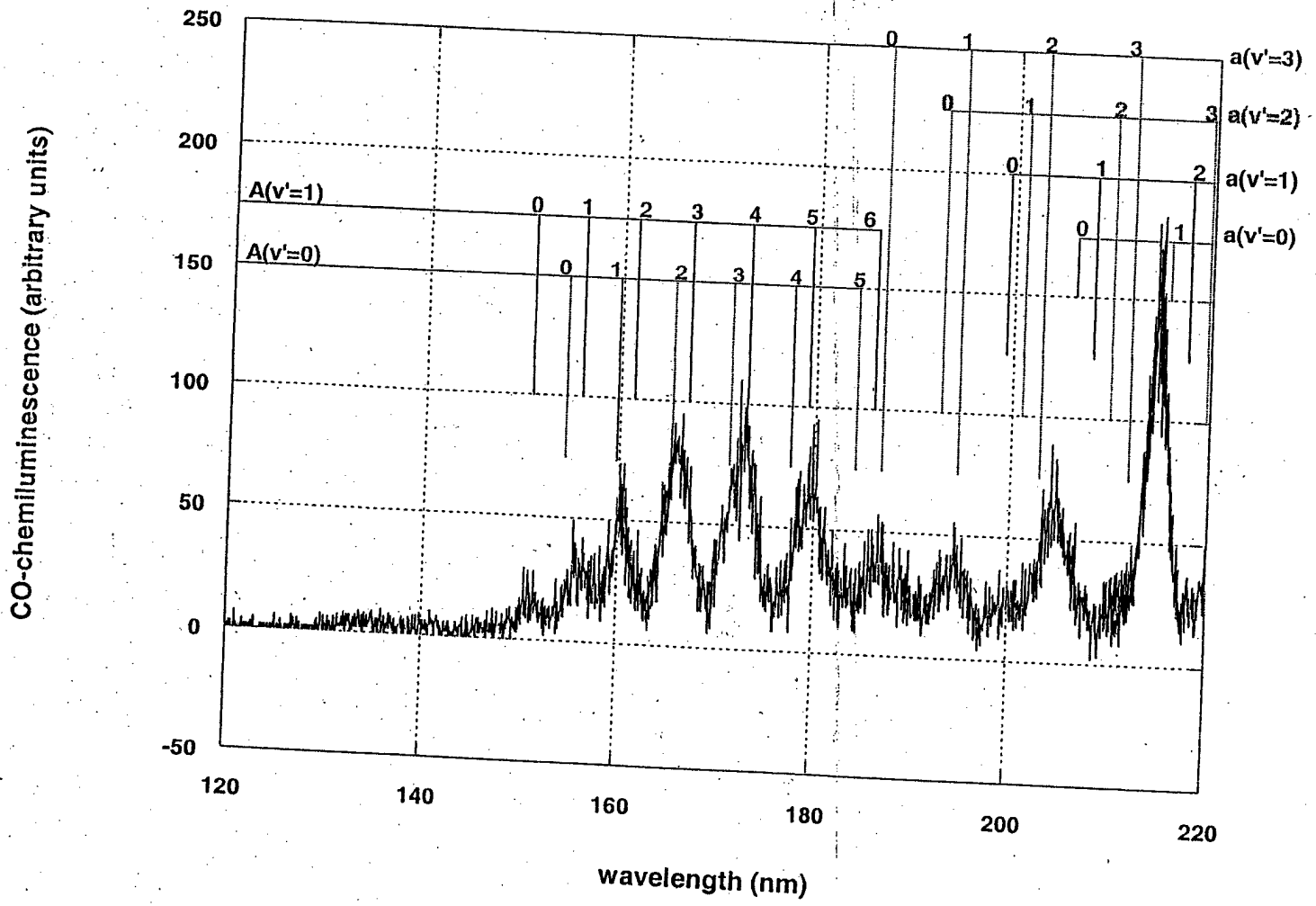
CO-chemiluminescence (arbitrary units)
250
200
150
100
50
0
-50
120
140
160
180
200
220
wavelength (nm)
A(v'=1)
A(v'=0)
a(v'=3)
a(v'=2)
a(v'=1)
a(v'=0)

Figure 2

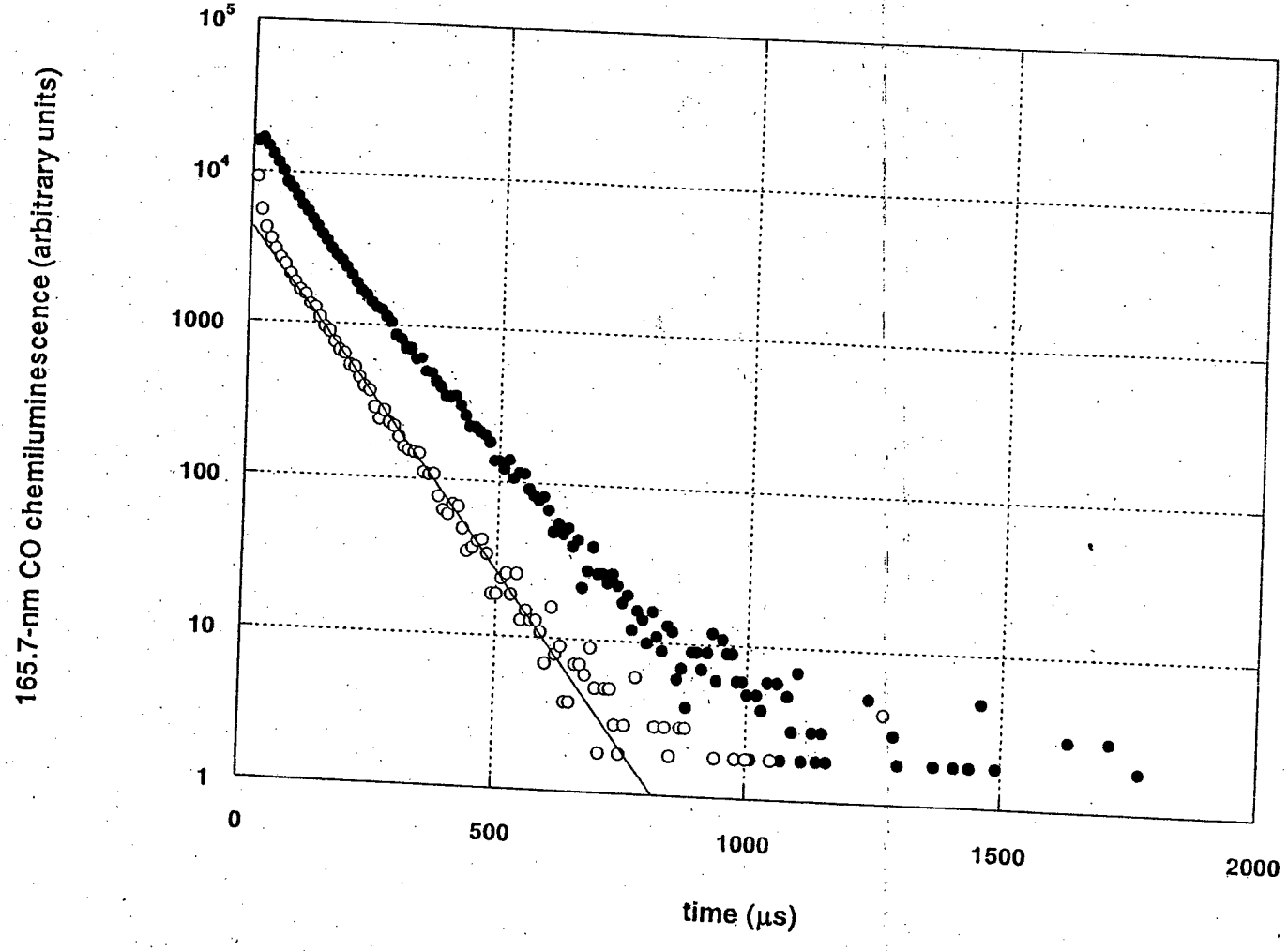
165.7-nm CO chemiluminescence (arbitrary units)
10^5
10^4
1000
100
10
1
0
500
1000
1500
2000
time (μs)

Figure 3

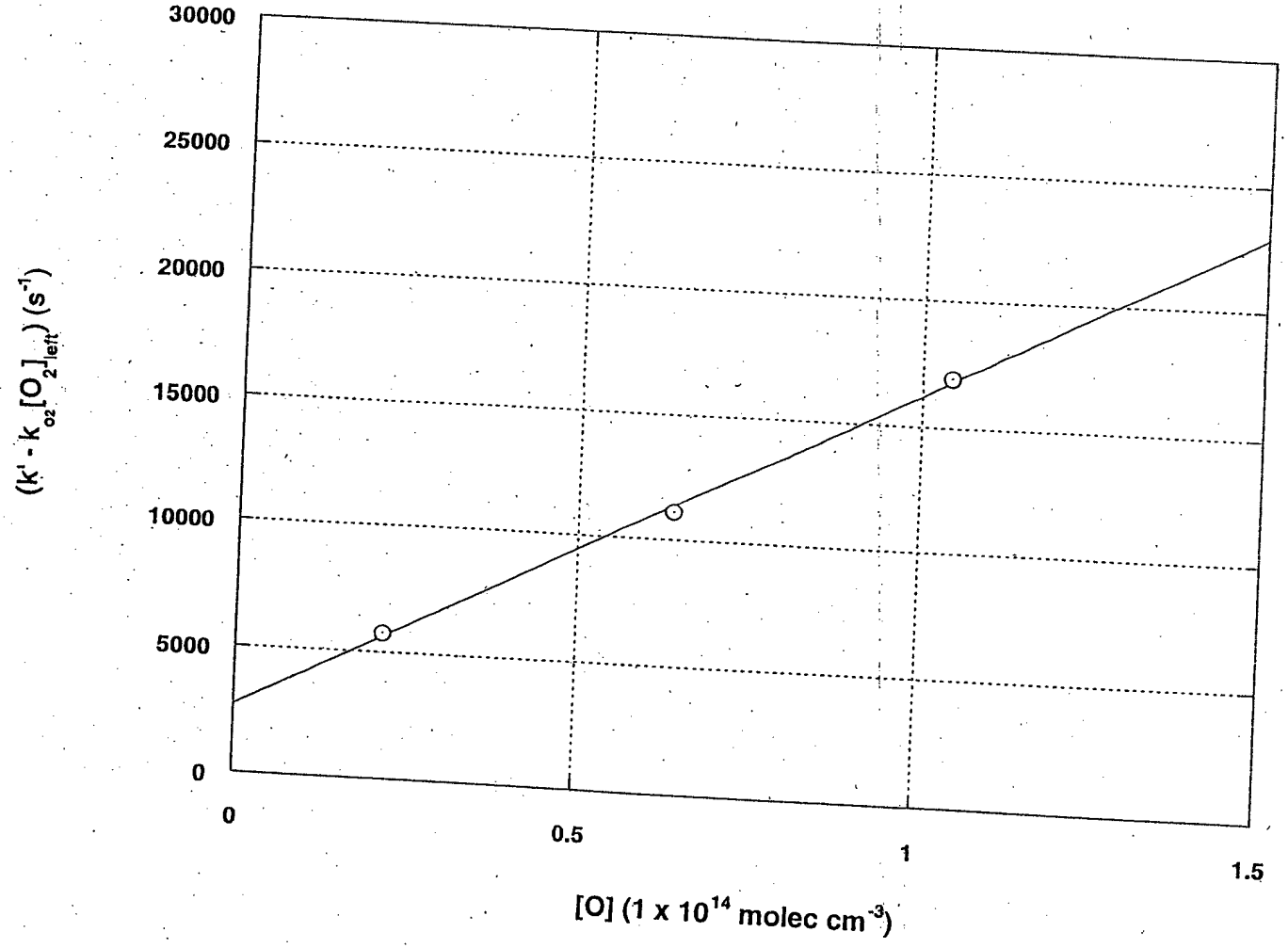
30000
25000
20000
15000
10000
5000
0
0
0.5
1
1.5
$(k' - k_{o2}[O_2]_{left})$ (s^{-1})
[O] (1 x 10^{14} molec cm^{-3})

Figure 4

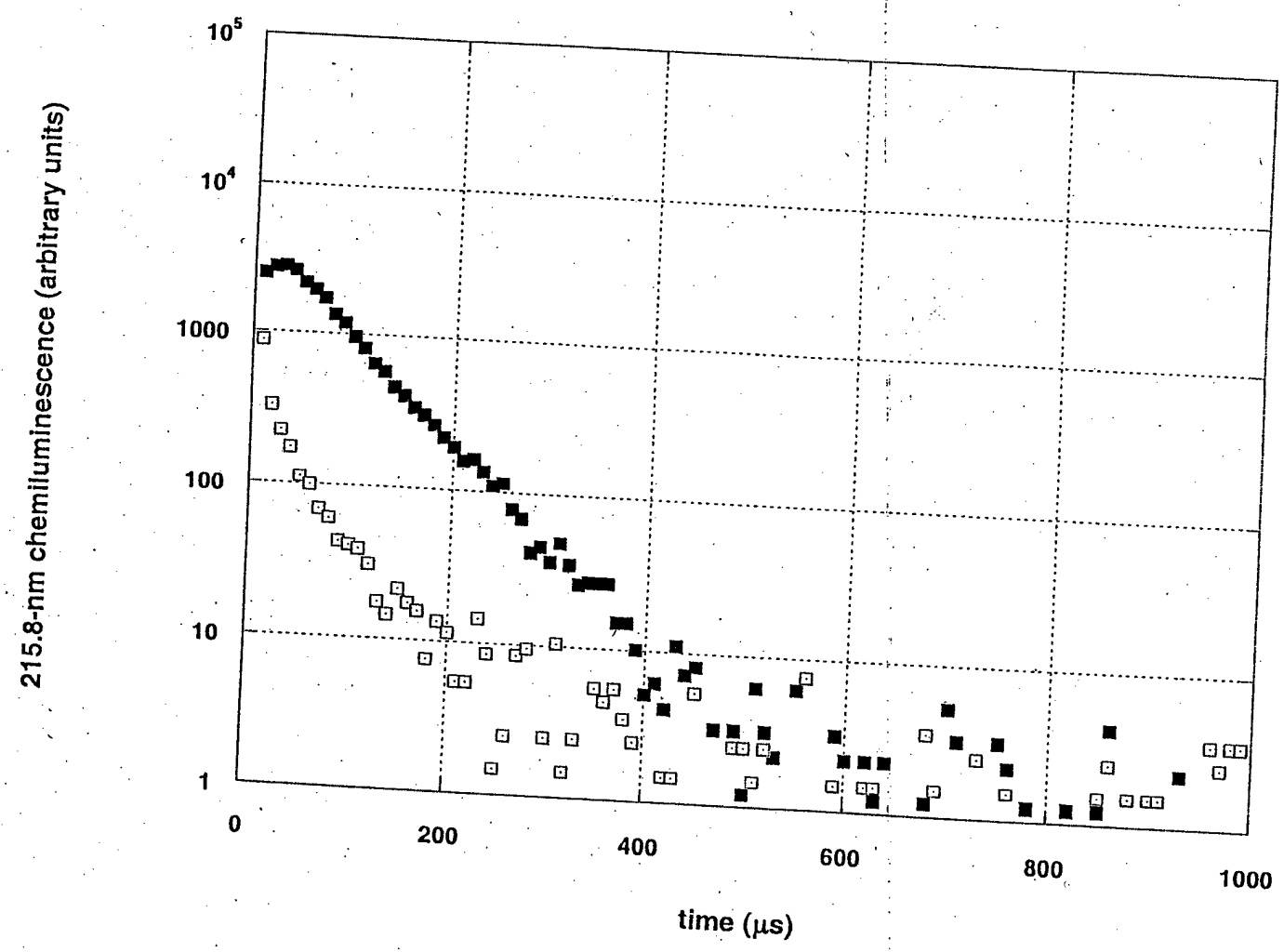
215.8-nm chemiluminescence (arbitrary units)
10^5
10^4
1000
100
10
1
0
200
400
600
800
1000
time (μs)

Figure 5

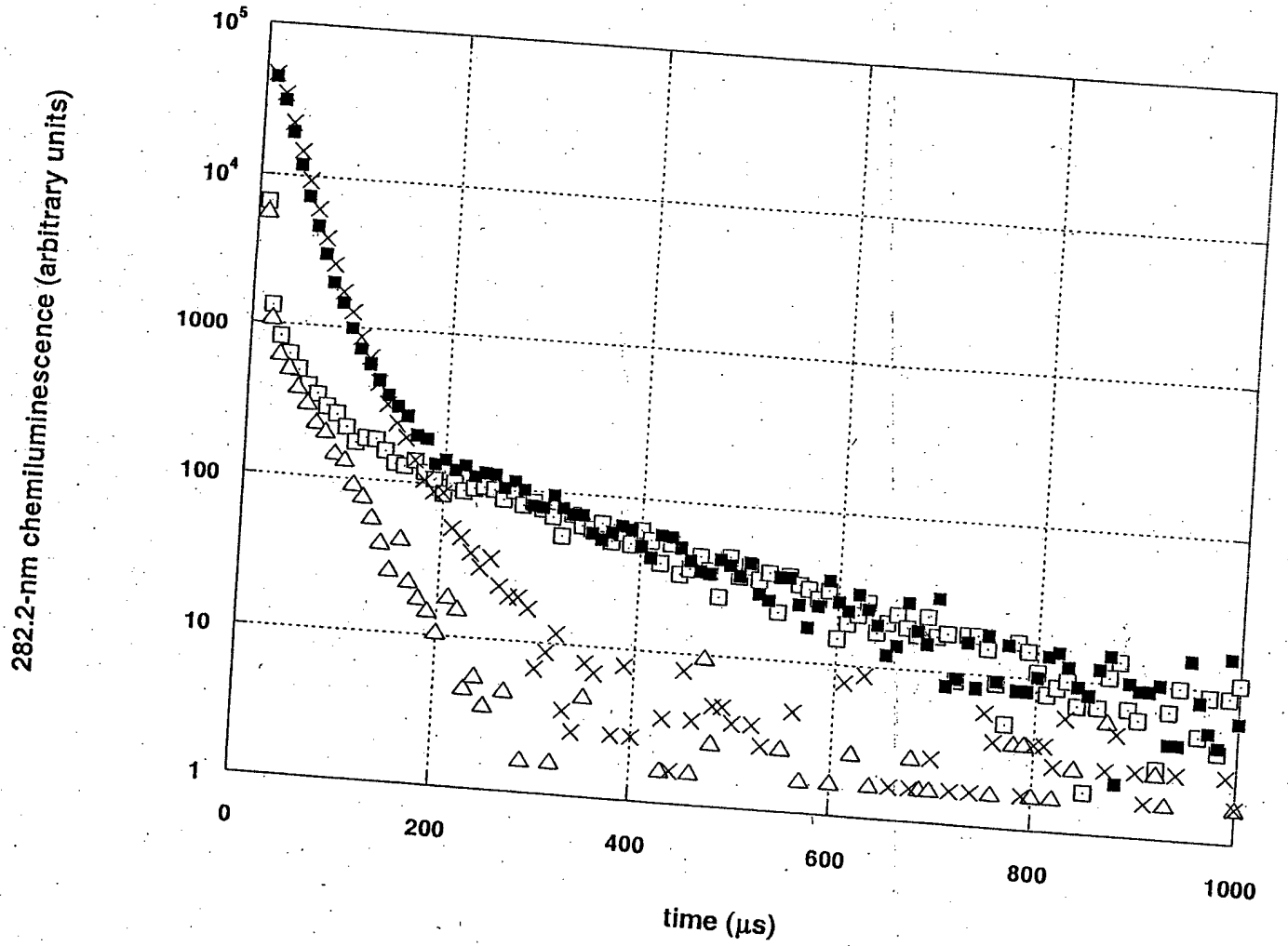
282.2-nm chemiluminescence (arbitrary units)
10^5
10^4
1000
100
10
1
0
200
400
600
800
1000
time (μs)

Figure 6

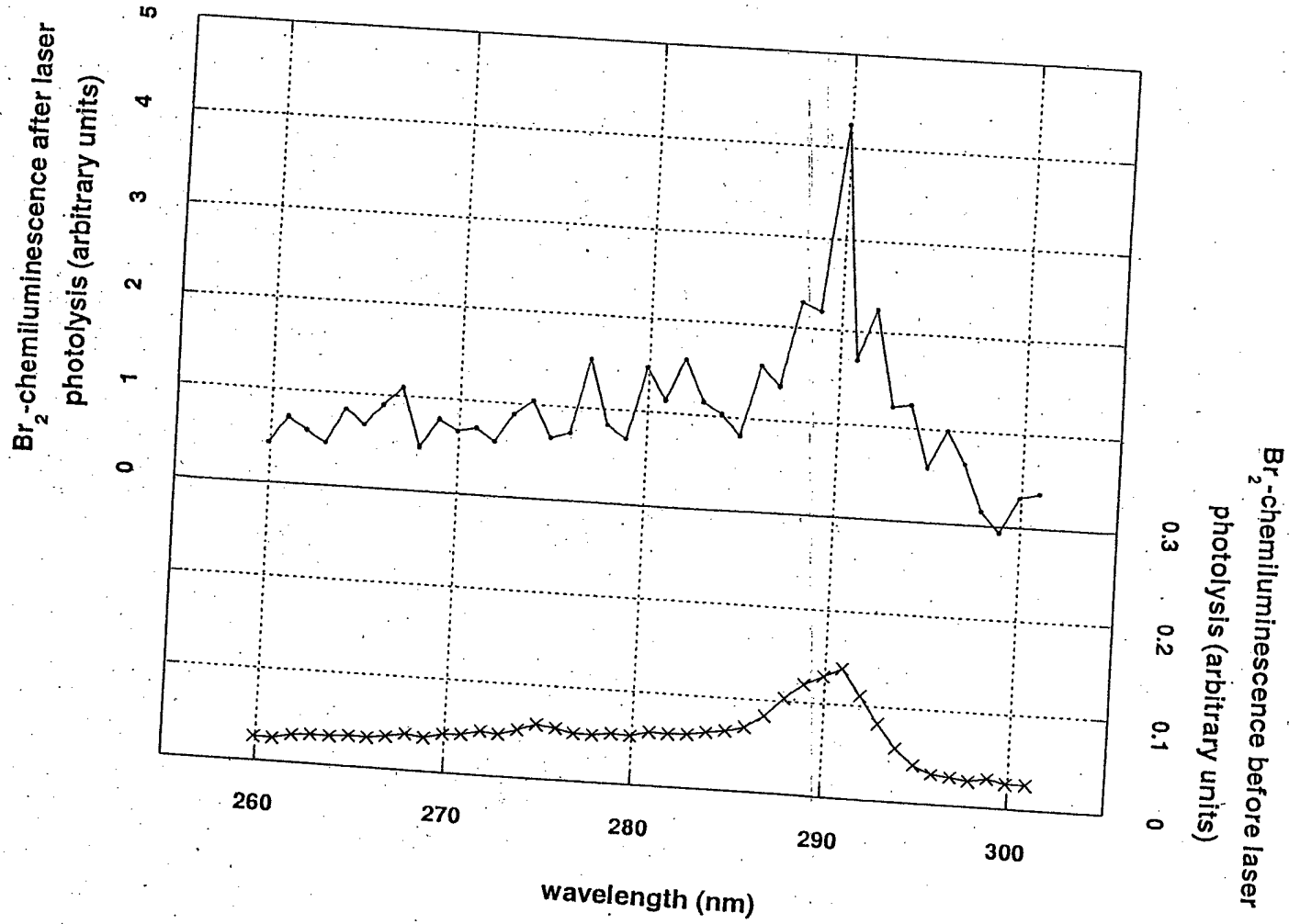
Br2-chemiluminescence after laser photolysis (arbitrary units)
0
1
2
3
4
5
260
270
280
290
300
wavelength (nm)
Br2-chemiluminescence before laser photolysis (arbitrary units)
0
0.1
0.2
0.3

Figure 7

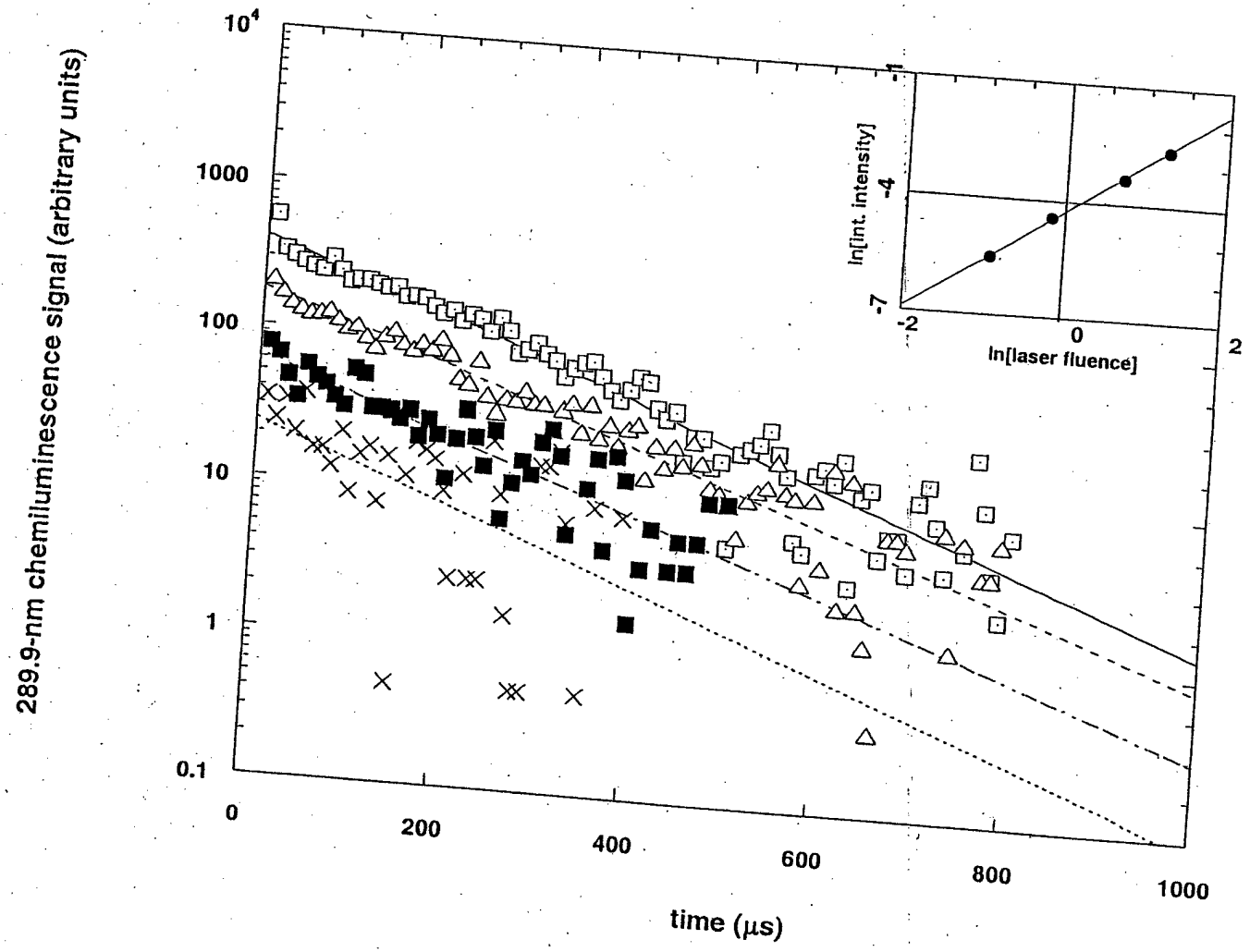
289.9-nm chemiluminescence signal (arbitrary units)
10^4
1000
100
10
1
0.1
0
200
400
600
800
1000
time (μs)
ln[int. intensity]
-1
-4
-7
-2
0
2
ln[laser fluence]

Figure 8

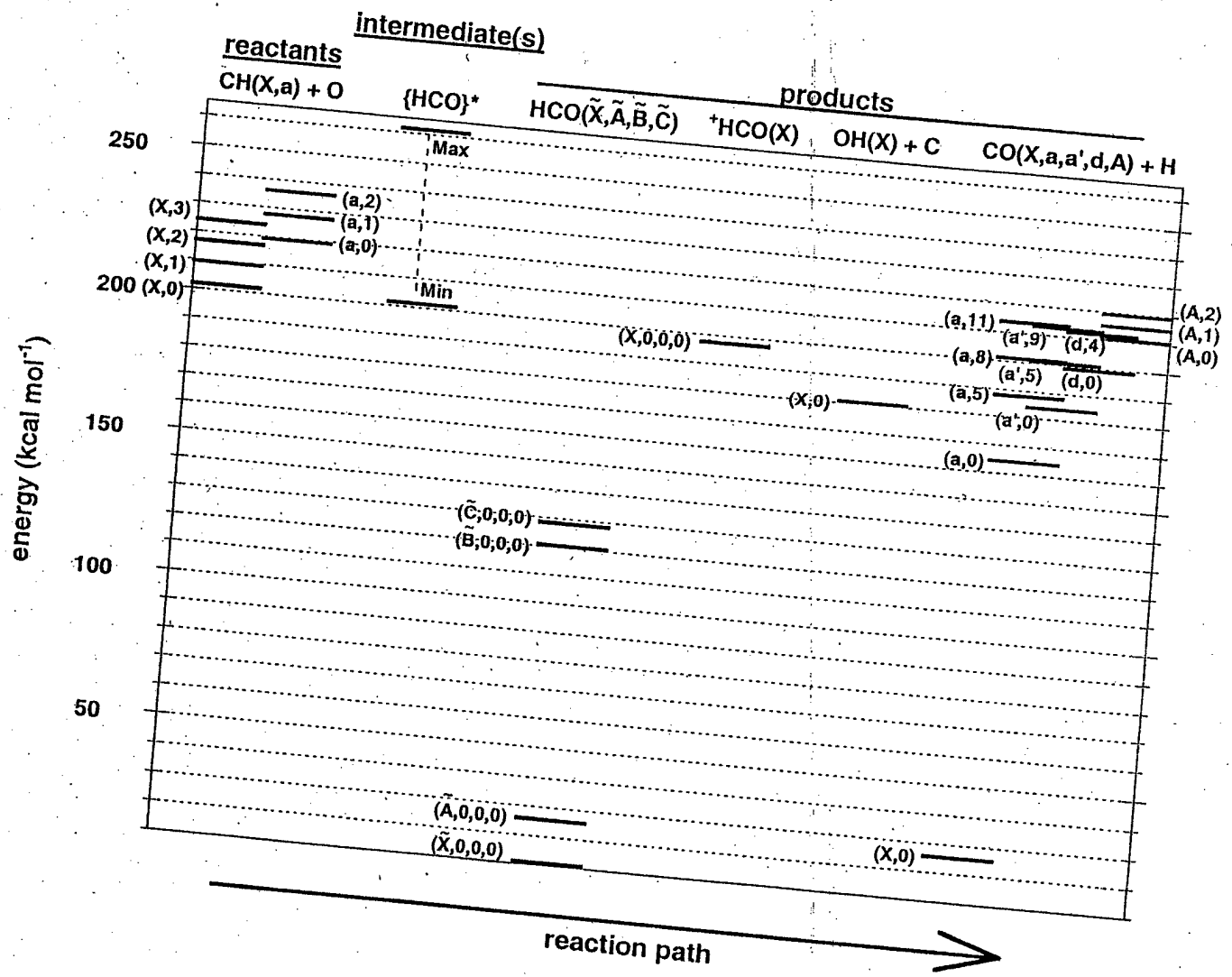
reactants
intermediate(s)
products
CH(X,a) + O
{HCO}*
HCO(X̃,Ã,B̃,C̃)
⁺HCO(X)
OH(X) + C
CO(X,a,a',d,A) + H
energy (kcal mol⁻¹)
250
200
150
100
50
Max
Min
(X,3)
(X,2)
(X,1)
(X,0)
(a,2)
(a,1)
(a,0)
(X,0,0,0)
(X,0)
(a,11)
(a',9)
(d,4)
(a,8)
(a',5)
(d,0)
(a,5)
(a',0)
(a,0)
(A,2)
(A,1)
(A,0)
(C̃;0;0;0)
(B̃;0;0;0)
(Ã,0,0,0)
(X̃,0,0,0)
(X,0)
reaction path